



Analysis of longitudinal wrinkle formation during calendering of NMC811 cathodes under variation of different process parameters

Ann-Kathrin Wurba¹ · Lennart Altmann¹ · Jürgen Fleischer¹

Received: 14 August 2023 / Accepted: 12 December 2023
© The Author(s) 2024

Abstract

The requirements for the lithium-ion battery (LIB) are constantly increasing. In the nearer future, batteries need to be even more powerful, safer and cheaper. One lever is the optimization of the production in order to minimize production scrap rates. In electrode manufacturing, calendering is an essential process step to adjust the volumetric energy density. However, this process leads to undesirable defects that result in production scrap. In this paper, the formation of longitudinal wrinkles is analyzed using a statistical experiment design. Electrode density, web tension and temperature are varied in two levels during calendering and are examined for their significance with regard to the geometry of the longitudinal wrinkles. Furthermore, the strain and the deformation of the electrode are analyzed. A complex interaction of material and process is revealed with respect to the formation of longitudinal wrinkles. A better understanding of these interactions contributes to optimize the calendering process and to find a solution to avoid longitudinal wrinkles.

Keywords Lithium-ion battery · Electrode production · Calendering · Longitudinal wrinkling

1 Introduction

Today's requirements for lithium-ion batteries and the associated challenges include not only high energy and power densities, but also safety issues and, at least, costs. In order to meet these requirements, this technology needs to be continuously improved. There are complex relationships between cell properties, materials and production, among other factors, that are not yet fully understood. Over 70% of the total manufacturing costs of a cell are related to the material, while the cathode accounts for almost 50% of these costs. Material scrap caused by electrode manufacturing defects are therefore cost-intensive. [1]

Calendering is of particular importance to achieve a high volumetric energy density, which is directly related to battery performance [2]. Furthermore, it influences the mechanical properties and the conductivity [3]. High line loads are required for high volumetric energy densities, that induce mechanical stresses in the electrode, which lead to

the formation of defects. These defects can occur in both coated and uncoated current collector and negatively affect the material quality as well as the web handling and therefore the productivity. So far, various calendering defects and challenges have been observed, while an initial overview can be found in [4]. The defects relevant to this work are described as follows. One approach to characterize deformations in wave and bulge shape, which are also referred to as corrugations, is the so-called defect evaluation index (DEI). It is calculated from the largest difference between the maximum and minimum amplitude. [5] High compaction rates lead to an increasing DEI [6]. The deformations depend on the thickness of the current collector and the material stiffness [7]. Looking at the metal foil industry shows that waves occur during the rolling of metal foils, if the parallelism of the rolls deviates by only a few hundredths of a millimeter and when the global web tension falls below a critical value. This critical value depends on the residual stresses in the material. If the distance between the rollers increases in the direction of the web edge, central waves occur and if the distance decreases in the direction of the web edge, waves are observed at the edge. [8] Small wrinkles at the coating edge, also known as foil embossing, are described in [9]. Embrittlement of the electrodes is also challenging, as it can cause web tears [4].

✉ Ann-Kathrin Wurba
ann-kathrin.wurba@kit.edu

¹ Institute of Production Science (wbk), Karlsruhe Institute of Technology (KIT), Kaiserstr. 12, 76131 Karlsruhe, Germany

The focus of this work is the analysis of the longitudinal wrinkle defect pattern, that occurs during calendering when a calendered web passes over a deflection roller under high web tension. An example of a forming longitudinal wrinkle is presented in Fig. 1 in Sect. 2.1. The point pattern is required for strain measurement. This defect is a plastic deformation in the shape of a wrinkle that forms parallel to the coating edge. It is characterized by its geometry, which is described by the height and the width of the longitudinal wrinkle as well as the distance between the longitudinal wrinkle and the coating edge, also referred to as position of the longitudinal wrinkle. Further details on the geometric description of longitudinal wrinkles are given in [10]. Longitudinal wrinkles are challenging, because they can easily cause web tears, resulting in scrap and production downtime [10]. They are also known in metal foil processing, where they are mainly analyzed by simulation. Longitudinal wrinkles are the result of a critical tension being exceeded. As the web moves, additional frictional forces are generated, that induce compressive stresses. In combination with the high web tension, this is the basis for the formation of longitudinal wrinkles. [11] Furthermore, similar phenomena are known that are referred to as buckling of stretched strips. A critical tensile stress induces lateral compressive stresses in a clamped strip that lead to wrinkling effects in the middle of metal or plastic strips. [12]

Moreover, small misalignments in the plane of the web can lead to the so-called in-plane bending. This effect also results into shear stresses, which can initially create troughs but also wrinkles. The same applies for changing deflection roller diameters. For a homogeneous web product the longitudinal wrinkles are created at a large angle to the running direction over the entire web width. [13] In [14] it is proposed that the compression stresses caused by misalignment can be compensated for by the systematic introduction of pre-tensile loading.

Reducing the formation of longitudinal wrinkles requires a deep understanding of the complex relationship between machine, process and material. With regard to the calendering of electrodes, no scientific work is known to date that investigates the formation of longitudinal wrinkles. Therefore, this paper presents the results of a full factorial experiment design with three factors and two levels. The experiment design is described in Sect. 2, while the results

Fig. 1 Formation of a longitudinal wrinkle with the coating edge on the left side



are presented and discussed in Sect. 3. Section 4 gives a short summary and outlook.

2 Experimental

This section provides a brief introduction to the electrode material used, the calendering machine as well as the sensor systems and gives a brief insight into the statistical evaluation.

2.1 Electrode material and equipment

All experiments were carried out using the lithium nickel manganese cobalt oxide (NMC811) cathode, that was also used in [10]. It is coated on both sides with a coating width of 155 mm and an uncoated part of 30 mm on each side. The density of the electrodes was calculated from the quotient of the areal weight of the coating of the electrode and the thickness of the coating of the electrode. To determine the thickness of the electrode, three circular samples each with a diameter of 18 mm were punched out on both sides of the electrode with the high precision electrode cutter EL-cut (EL-Cell GmbH) and measured with the digital indicator MarCator 1075R (Mahr GmbH). To obtain the thickness of the coating, the thickness of the substrate foil is subtracted. In this case the thickness of the aluminum substrate foil was 15 μm , which was taken from the manufacturer's specifications. Afterwards the areal weight of these samples was measured using the laboratory balance EW 220-3NM (KERN & SOHN GmbH). Again, the areal weight of the pure aluminum substrate is subtracted. The average thickness of the coating was 188.0 μm with a standard deviation of 0.89 μm while the average areal weight of the coating was 40.87 $\text{mg}\cdot\text{cm}^{-2}$ with a standard deviation of 0.63 $\text{mg}\cdot\text{cm}^{-2}$ which results into an average density of 2.17 $\text{g}\cdot\text{cm}^{-3}$.

Calendering was performed on the calender GKL 500 MS (Saueressig Group), that was already introduced in [10]. The most relevant process parameters for this study are the line load F_L , the web tension F_W and the temperature T of the rollers. The density ρ is set via the line load, with a maximum line load of 2000 $\text{N}\cdot\text{mm}^{-1}$ at a maximum coating width of 350 mm for this calender. The schematic experiment setup is shown in Fig. 2. The web tension is adjusted individually via the unwinder, rewinder and the tension unit and varies between 1 N and 250 N. The temperature limits for the calender rollers are room temperature and 90 °C.

2.2 Experiment design and statistical evaluation

The experiments were planned with the help of the statistical software Minitab® (Minitab, LLC). Table 1 presents the chosen coded full factorial experiment design with the

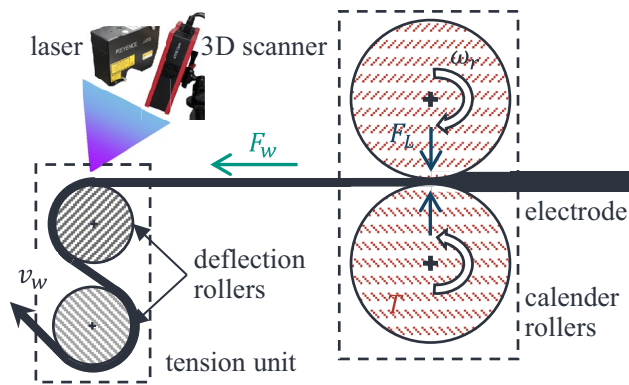


Fig. 2 Experiment setup with the sensors, the web speed v_w , the angular speed of the rollers ω_r , the temperature T of the rollers, the line load F_L and the web tension F_w [10]

Table 1 Coded full factorial experiment design

No.	ρ	F_w	T
#1	+1	-1	-1
#2	-1	+1	-1
#3	-1	-1	+1
#4	+1	+1	+1
#5	-1	+1	+1
#6	+1	+1	-1
#7	-1	-1	-1
#8	+1	-1	+1

Table 2 Factor levels

Factor	-1	+1
Density (ρ)/g cm ⁻³	2.8	3.3
Web tension (F_w)/N	80	110
Temperature (T)/°C	30	90

three factors density (ρ), web tension (F_w) and temperature (T) and the two levels shown in Table 2. In this context, the web tension corresponds to the web tension at the tension unit, which can be set independently of the web tension at the winder and unwinder. The tension unit is schematically displayed in Fig. 2. For simplicity, the web tension at the tension unit will be referred to in the following as the web tension. All experiments were performed at a web speed of 1 m min⁻¹ and a web tension of 60 N for unwinder and rewinder. It was investigated whether the three factors have a significant influence on the geometry of the longitudinal wrinkles. From metal strip conveying, there is a presumption that a minimum web tension must be applied for the longitudinal wrinkles to form [11]. To verify this, two additional experiments were carried out with the lower web tension $F_w = 60\text{N}$ at the high density of 3.3 g cm⁻³ and the two temperature levels of 30 and 90 °C. However, these experiments

are not part of the experiment design and are therefore not included in the results.

The geometry information from the laser and 3D scanner data were statistically analyzed in Minitab as well. For the generation of the factorial regression from the process parameters and the geometry information, the two-sided confidence level had to be selected at 90 %, since otherwise no model could be obtained and thus no evaluation would have been possible. This corresponds to a significance level of $\alpha = 0.1$. However, the correlations between the three factors and the line load, strain and deformation could be determined at the 0.05 significance level. All regression models were built via backward elimination. In the Minitab software, this requires only the specification of α . For backward elimination, the model first contains all terms that are eliminated step by step. The process is terminated once all variables with a probability- (p) value greater than α have been removed. [15] It is possible to exclude terms for the initial model, but in this case all terms were allowed up to order 3, which corresponds to the triple interaction of density, temperature, and web tension. The results of the statistical evaluation from Minitab are presented in Sect. 3 using main effects plots, in which the mean values of the individual levels are displayed and connected by a line. The strength of an effect is indicated by its magnitude. The significance of the effects is determined using the p -values. [16] Factors that are not significant and also do not exist in the regression model are shown in grey in the main effects plots.

3 Results and discussion

The influence of calendaring on the electrode as well as on the geometry of the longitudinal wrinkles is described and discussed below. Longitudinal wrinkles were observed in all experiments. Their geometric values are shown in the Appendix in Fig. 15.

However, it is to be noted, that longitudinal wrinkles were only formed at irregular intervals in the experiment #7. At this point, the test area is at the limit of stable longitudinal wrinkle formation. In the two additional experiments carried out with the lower web tension $F_w = 60\text{N}$ no longitudinal wrinkle formed. This confirms that a critical web tension must be exceeded for longitudinal wrinkles to form. This was also shown for hard carbon anodes in [10]. The entire electrode is pressed less strongly against the deflection roller at a lower web tension. Figure 3 illustrates the surface pressure F_{SP} resulting from the web tension schematically. On the one hand, the electrode has greater freedom of movement transverse to the running direction, i.e. in the x -direction. The uncoated part of the substrate may move minimally and thus relax. On the other hand, the coated part is also pulled less strongly against the deflection roller, so that there may

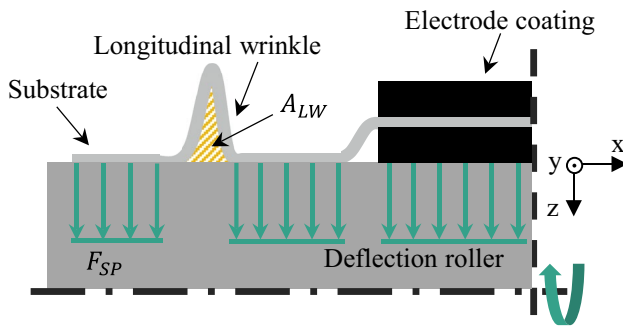


Fig. 3 Schematic illustration of the longitudinal wrinkling during deflection with the schematic surface pressure F_{SP} and the area of the longitudinal wrinkle A_{LW} in yellow

still be minimal voids between the coating and the deflection roller. Thus, a compensating movement in the form of a longitudinal wrinkle to compensate for the deformation is not necessary. In the following, the wrinkle area A_{LW} is introduced for better illustration. It is marked in yellow in Fig. 3 and describes the free area between the longitudinal wrinkle and the deflection roller. It depends on the width and height of the wrinkle. A larger A_{LW} results in a larger proportion of wrinkled uncoated substrate.

The influence of calendering on the electrode's behavior is discussed in the subsection below, followed by the evaluation of the geometry of the longitudinal wrinkles.

3.1 Influence of calendering on the electrode's behavior

In the following subsections the results for the line load, strains and deformations are shown and discussed.

3.1.1 Line load during calendering

The compaction of the porous coating in the calendering process requires high line loads. The experiments with the lower density of 2.8 g cm^{-3} needed an average line load of 539.66 N mm^{-1} with a standard deviation of 63.88 N mm^{-1} . The higher density of 3.3 g cm^{-3} needed an increase of the average line load to $1874.58 \text{ N mm}^{-1}$ with a higher standard deviation of 199.58 N mm^{-1} . The density therefore has a positive effect and also the analysis of variance demonstrated, that the factor density is significant with $p = 0.00001$ at a level of significance of $\alpha = 0.05$. Furthermore, the analysis of variance showed that the factor temperature is significant with $p = 0.02713$ and it has a negative effect. The two-way interaction between temperature and density is also significant with $p = 0.02311$ and also has a negative effect for the high density. At the lower density, the effect of the temperature is not as clear. This result confirms, that calendering to a high density at higher temperatures requires

a lower line load [17] and it also explains the existing standard deviation of the line loads especially for the high density.

3.1.2 Strain caused by calendering

During calendering the coating of the electrode is compacted and therefore strains are induced. This has already been shown in [18], where Mayer et al. also found that the density has a positive effect on the strains in the running direction (in the following referred to as y -strain) and transverse to the running direction (in the following referred to as x -strain). In this paper the variance analysis could prove this statement. The results of the individual experiments are displayed in Fig. 12 in the Appendix. As shown in Fig. 4, the density has a significant positive influence on x -strains with $p = 0.0441$ and, as displayed in Fig. 5, also on the y -strains with $p = 0.0006$ at a level of significance of $\alpha = 0.05$. The factor temperature is not significant, but has a medium negative effect on the x -strains and a small negative effect on the y -strains. The decreasing strains with increasing temperature are explained by the assumption that the coating material softens somewhat at higher temperatures and is therefore easier to deform. For example, in [19] this is attributed to the temperature-dependent shear behavior of the Polyvinylidene fluoride (PVDF) binder. Although, the deformation in the x - and y -direction decreases, but is possibly replaced by the stronger deformation in the z -direction. This supports the

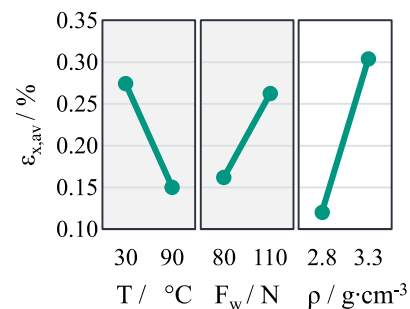


Fig. 4 Main effects plot for the average x -strain $\epsilon_{x,av}$

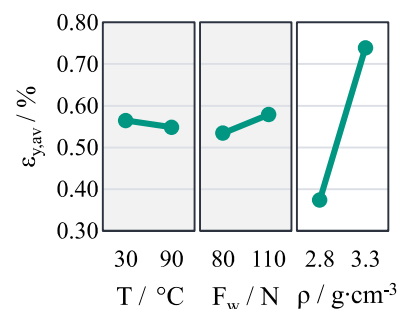


Fig. 5 Main effects plot for the average y -strain $\epsilon_{y,av}$

theory for the reduced line loads at higher temperatures. It is also possible that the heated electrode material relaxes somewhat after calendaring, so that the x - and y -strains tend to be less prominent. The web tension has a negative effect on the strains, which is also not significant. Furthermore, the main effects plots and Fig. 12 in the Appendix show that the y -strains are higher than the x -strains, which was also observed by Mayer et al. [18]

3.1.3 Deformation caused by calendaring

It is assumed that the coated part of the electrode elongates and thus the compensating movement occurs directly after calendaring in the shape of a deformation or, for the NMC811 cathodes, in the shape of a wave. The wave geometry is characterized by its amplitude and wavelength. The results of each experiment can be taken from Figs. 13 and 14 in the Appendix. Only the density has a significant positive effect on the amplitude of the wavy electrode with $p = 0.0106$, which is shown in Fig. 6. As already described in the previous section, the strains force the coating to be stronger displaced in x - and y -direction with increasing density. This causes an elongation of the coated part of the electrode and therefore a higher amplitude. This was also observed by [6]. In addition, as described in the introduction in [8], in metal foil processing there is the phenomenon of wave formation when the roll gap is not parallel and the line load is distributed inhomogeneously. The zones that are more compressed due to the reduced roller gap form waves. In this case, the coating is compacted due to the greater thickness, while the uncoated substrate has no contact to the rollers and is therefore not compacted. The adhesion of the coating on the substrate is strong enough, that the waves form across the web width without delamination. The calender rollers bend due to the high roll-bending force when the line load is applied to the electrode, so that the roll gap is larger towards the inside [20]. This creates waves at the edges of the electrode, which can superimpose the waves across the web width. However, this superposition

complicates the evaluation of wavelength and amplitude and it has to be noted that the analysis of deformation in this paper is based on few data. The data acquisition and processing will be optimized in the future to generate more valid statements. In contrast, the wavelength is only significantly influenced by the web tension with $p = 0.0352$ and a positive effect, as shown in Fig. 7, which was also found by [6]. In [8] it is also shown, that the web tension has an influence on the formation of the waves and a high web tension reduces the wave formation. However, the findings on wave formation in metal foils do not include the factor of coating of the electrode. Therefore, an additional explanation is, that the high web tension pulls the electrode so strongly in the running direction that the waves are already pulled apart during formation. This results in the peaks and valleys of the deformed electrode hitting the deflection roller at less frequent intervals. The coated part of the electrode can better contact the deflection roller, since waves with the same amplitude, but longer wavelength and assuming the same stiffness are less steep.

3.2 Influence of calendaring on the geometrical characteristics of a longitudinal wrinkle

A high density leads to high strains and high amplitudes as described in Sect. 3.1. Since the coated part of the electrode has stretched and elongated, a large part of the web tension is on the unelongated and uncoated edges of the electrode. The electrode is thus limited in its freedom of movement transverse to the running direction when it hits the deflection roller due to the pressed edges as illustrated in Fig. 3. Furthermore, it is assumed that the electrode contracts somewhat towards its center in the area between the calendaring rollers and the deflection roller and that the effect of bulging is intensified. This was not measured so far, but when examining the investigations with the sheets that are clamped on both sides and subjected to tensile loads, where wrinkles occur in the middle [12], the sheet must be pulled to the center due to material preservation. During deflection, the

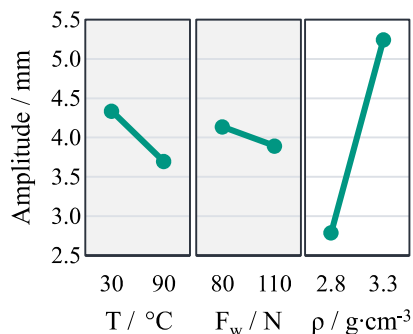


Fig. 6 Main effects plot for the amplitude

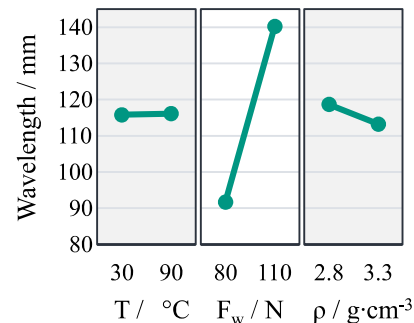


Fig. 7 Main effects plot for the wavelength

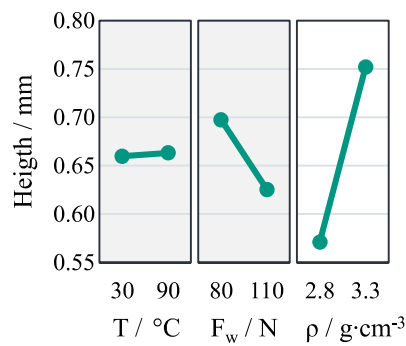


Fig. 8 Main effects plot for the height

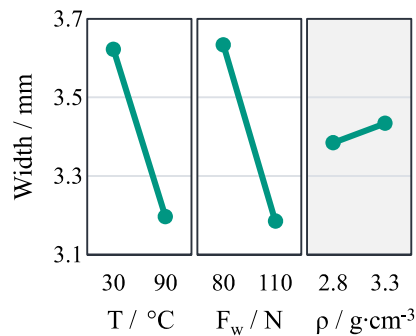


Fig. 9 Main effects plot for the width

coated and deformed part of the electrode is forced to nestle against the deflection roller by the high web tension. Due to the lateral limitation, the bulged material is compensated by the formation of a longitudinal wrinkle. The coating stiffens during calendaring and does not allow longitudinal wrinkles to form, which is why the longitudinal wrinkles form in the uncoated edge area. In the following subsections the influence of the varied process parameters on the geometrical characteristics of a longitudinal wrinkle are discussed. Figures 8, 9 and 11 display the main effects plots for the statistical evaluation. The overview of the results of all individual experiments is presented in Fig. 15 in the Appendix. This overview shows that the associated standard deviations for the individual experiments for height and width are small. The distance shows higher standard deviations, which is discussed in the corresponding section.

3.2.1 Influence on the height of a longitudinal wrinkle

The main effects plot in Fig. 8 shows the statistic evaluation of the influence of density, web tension and temperature on the height of a longitudinal wrinkle. Only the factor density is significant with $p = 0.082$ at a level of significance of $\alpha = 0.1$. It has a positive effect, so the height of the longitudinal wrinkle is increasing with the density. All other

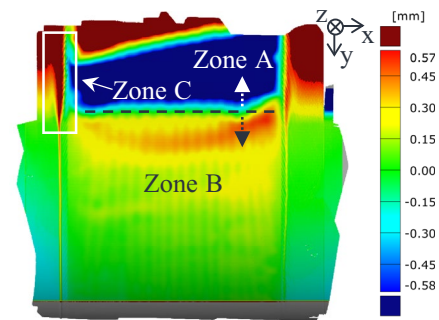


Fig. 10 3D Scan of the electrode as it hits the deflection roller

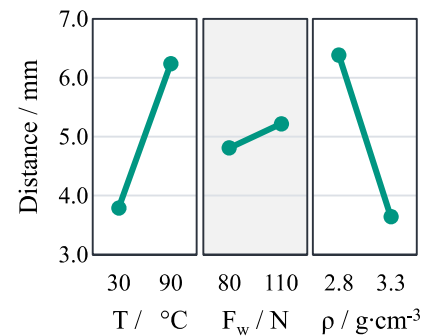


Fig. 11 Main effects plot for the distance

factors as well as the two- and three-way interactions are not significant. The main effects plot also shows, that the temperature has almost no influence on the height, while the web tension has a medium effect. With increasing density, the amplitudes of the waves are higher, so more material is displaced, which must be compensated by the wrinkle. This results in an increase in the height of the longitudinal wrinkle and, taking into account the non-significant increase in width, an increase in the wrinkle area A_{LW} .

3.2.2 Influence on the width of a longitudinal wrinkle

As shown in the main effects plot in Fig. 9, the factor web tension is significant with $p = 0.0049$ and has a negative influence, while the factor temperature has a negative significant effect with $p = 0.059$ as well. Lastly there is the significant and likewise negative two-way interaction between web tension and temperature with $p = 0.0525$. Therefore, the width decreases with increasing web tension and increasing temperature and the longitudinal wrinkle becomes narrower. The density and its two-way interactions as well as the three-way interaction do not have any significant effect. At higher web tensions, the uncoated substrate is pressed more strongly onto the deflection roller, which limits the freedom of movement of the electrode on the deflection roller more strongly

transverse to the running direction. Figure 10 shows a 3D scan of the top view of the electrode hitting the deflection roller. Zone A describes the electrode part that is still running freely, while in zone B the electrode is pressed against the deflection roller. Zone C marks the formation area of longitudinal wrinkles. It is located on both sides of the electrode in the same area, but in Fig. 10, it is shown only on one side for clarity. The initial longitudinal wrinkle is much wider before hitting the deflection roller, as visible in zone C of Fig. 10. Directly at hitting the deflection roller, probably there is already such a high limiting force, because of the surface pressure F_{SP} , as shown in Fig. 3. Thus, the longitudinal wrinkle cannot spread out to the side and remains narrow. A high web tension also leads to lower longitudinal wrinkles, as mentioned in the previous section, even though this effect is not significant. So, at higher web tension, a wrinkle tends to have a lower wrinkle area A_{LW} , as this is the more stable condition compared to a larger wrinkle area. When the electrode touches the deflection roller, it has already cooled down. The temperature therefore has no direct influence on the shape of the longitudinal wrinkle. However, it is assumed that it influences the material properties, such as the bending stiffness, and thus have an influence on the width of the longitudinal wrinkle in a way, that has to be investigated in further studies.

3.2.3 Influence on the position of a longitudinal wrinkle

As already described in Sect. 1 the position of the longitudinal wrinkle is defined as the distance between the longitudinal wrinkle and the coating edge. Significant influence factors on the distance are the density with $p = 0.0476$ and the temperature with $p = 0.0675$. As shown in Fig. 11 the distance is decreasing with increasing density, which is referred to a negative effect. The temperature has a positive effect, which means that the distance is increasing with increasing temperature. All other factors and interactions are not significant. As already discussed in the sections before, the area of the longitudinal wrinkle A_{LW} increases with increasing density and therefore a larger proportion of the uncoated substrate is wrinkled. It is conceivable that this larger longitudinal wrinkle is more inert than smaller longitudinal wrinkles and is therefore located closer to the coating. This is consistent with the influence of the web tension, although it is not significant. An increasing web tension leads to a decreasing wrinkle area A_{LW} and thus to a shorter distance. The significant effect of temperature is attributed to a change in material behavior, analogous to the influence on width, discussed in the previous subsection. Although the process parameters show strong effects on the position of the longitudinal wrinkles, it must be noted that the position of the longitudinal wrinkles changes during their lifespan. According to previous observations, the wrinkle forms, moves to a certain position, remains stable for a while and then runs out again. It is assumed that the surface

pressure caused by the web tension prevents the wrinkle from running out to the edge of the web. However, the time spent in the stable state and thus the length of the longitudinal wrinkles has not yet been investigated and is the subject of future work. The migration of longitudinal wrinkles is also described in [13], but homogeneous webs are considered there and the phenomenon is not investigated further. The high standard deviations of the distances of the individual tests in Fig. 15 in the Appendix also indicate a migration of the longitudinal wrinkles, although only the data of the stable areas of the wrinkle were used. This shows that the distance also changes within one experiment. The mean values shown in the main effects plot therefore only provide an initial indication of the behavior of the longitudinal wrinkles.

4 Summary and outlook

First, it was confirmed that a high density is related to a high line load during calendering, since a compressive force is required for compaction. Further, it was identified that a high temperature results in a decrease of the line load, because the deformability of the coating is temperature-dependent. Calendering creates strains in the electrode, resulting in deformations. In the uncalendered state, the constant conveyance of the web without deviations from the stable state generally does not result in longitudinal wrinkles. The changed material behavior must therefore be partly responsible for the formation of the longitudinal wrinkles. Higher strains were found in the coated part of the electrode at the high density, because more material has to be displaced to achieve a higher density. For the same reason, the high density leads to higher amplitudes of the deformed and wavy electrode web. High densities therefore cause significant changes in the electrode behavior. The wave length increased with higher web tensions. This can be explained by the stretching effect of the tensile force already applied during the formation of the waves and is overlaid to a certain extent by the effect of wave formation at a non-parallel roll gap [8]. Concerning the characteristic geometry of the longitudinal wrinkles, it was shown that the higher density caused higher longitudinal wrinkles, as greater compensation of the displaced material and deformation is required. Furthermore, the higher density led to a lower distance between the longitudinal wrinkle and the coating edge, because higher densities generate a higher longitudinal wrinkle area A_{LW} . This makes the longitudinal wrinkle more inert under the high surface pressure F_{SP} and hinders the migration to the web edge. Temperature is significant and, when increased, it results in narrower longitudinal wrinkles, that have a greater distance to the coating edge. Since the electrode hits the deflection roller when cold, the temperature has an indirect influence via the material properties, which still needs to be investigated. Finally, the high web tension led to narrower longitudinal

wrinkles, because the high surface pressure during the formation of the longitudinal wrinkles prevents expansion. In addition, the wrinkles have a smaller area A_{LW} at high web tension in combination with a lower height. The wrinkle is therefore in a more stable state. The additional experiments with a lower web tension showed that a minimum web tension is needed to form longitudinal wrinkles. All in all, the relationship between the process parameters and longitudinal wrinkling is complex. In [6], for example, the formation of deformations in NMC622 and NMC811 was compared, which differ significantly. This is attributed to the material behavior and confirms the impression that the material behavior also has an influence on the formation of longitudinal wrinkles. Therefore, the material changes caused by calendering must be investigated. In the first step, this has already been started by analyzing the strains. Of particular interest is the bending behavior, which changes due to the stiffening of the electrode in the calendering process. This will be part of further investigations. Moreover, additional experiments with different materials should be carried out to further refine the findings. Due to this complex relationship, the development of an additional device, that reduces longitudinal wrinkles independently of the process variables and material properties is in progress.

Appendix

See Figs. 12, 13, 14 and 15.

Fig. 12 Results for the x- and y-strains

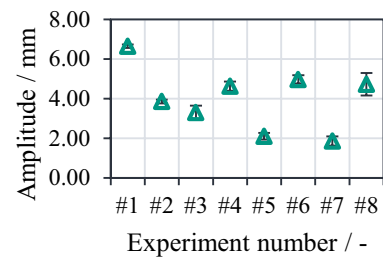
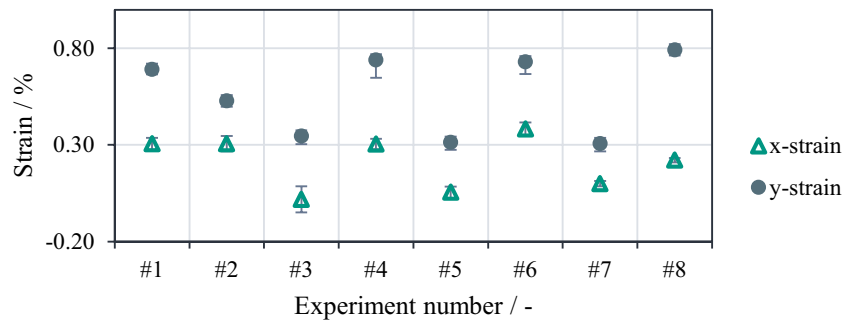


Fig. 13 Results for the amplitude

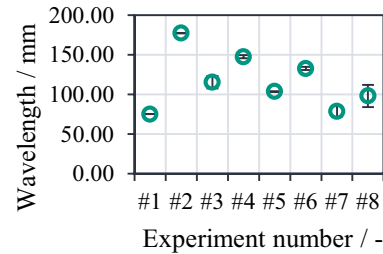
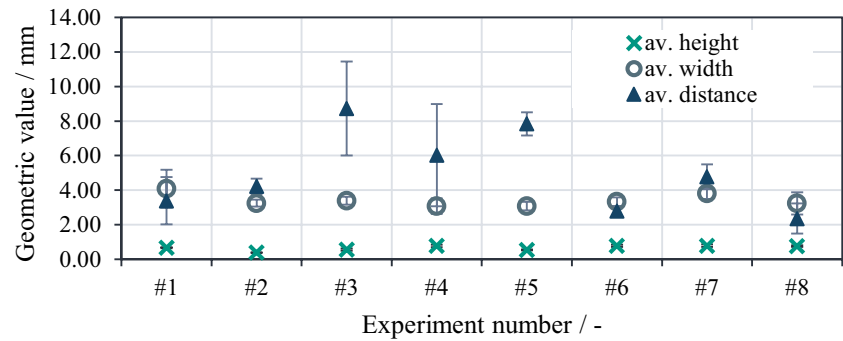


Fig. 14 Results for the wavelength

Fig. 15 Results for the geometrical values height and width of a longitudinal wrinkle and distance to the coating edge



Acknowledgements This research was funded by Deutsche Forschungsgemeinschaft (DFG, German Research Foundation) under Germany's Excellence Strategy—EXC 2154—project number 390874152 and by the Federal Ministry of Education and Research (BMBF), Project InteKal (grant number 03XP0348C). Furthermore, part of this work was done at the KIT Battery Technology Center (KIT-BATEC) and contributes to the research performed at CELEST (Center for Electrochemical Energy Storage Ulm-Karlsruhe). Furthermore, the authors would like to thank C. Reusch for processing the data in MATLAB.

Author contribution Ann-Kathrin Wurba: Conceptualization, Methodology, Software, Validation, Formal Analysis, Investigation, Data Curation, Writing – Original Draft, Visualization. Lennart Altmann: Software, Data Curation, Writing – Original Draft, Visualization. Jürgen Fleischer: Writing - Review & Editing, Supervision, Funding acquisition.

Funding Open Access funding enabled and organized by Projekt DEAL.

Data availability The data associated with this article is available at: <https://doi.org/10.5281/zenodo.10479389>.

Declarations

Conflict of interest The authors declare that they have no conflict of interest.

Open Access This article is licensed under a Creative Commons Attribution 4.0 International License, which permits use, sharing, adaptation, distribution and reproduction in any medium or format, as long as you give appropriate credit to the original author(s) and the source, provide a link to the Creative Commons licence, and indicate if changes were made. The images or other third party material in this article are included in the article's Creative Commons licence, unless indicated otherwise in a credit line to the material. If material is not included in the article's Creative Commons licence and your intended use is not permitted by statutory regulation or exceeds the permitted use, you will need to obtain permission directly from the copyright holder. To view a copy of this licence, visit <http://creativecommons.org/licenses/by/4.0/>.

References

- Kwade A, Haselrieder W, Leithoff R, Modlinger A, Dietrich F, Droeder K (2018) Current status and challenges for automotive battery production technologies. *Nat Energy* 3:290–300. <https://doi.org/10.1038/s41560-018-0130-3>
- Meyer C, Bockholt H, Haselrieder W, Kwade A (2017) Characterization of the calendaring process for compaction of electrodes for lithium-ion batteries. *J Mater Process Technol* 249:172–178. <https://doi.org/10.1016/j.jmatprotec.2017.05.031>
- Primo EN, Touzin M, Franco AA (2021) Calendaring of $\text{Li}(\text{Ni}_{0.33}\text{Mn}_{0.33}\text{Co}_{0.33})\text{O}_2$ -based cathodes: analyzing the link between process parameters and electrode properties by advanced statistics. *Batter Supercaps* 4:834–844. <https://doi.org/10.1002/batt.202000324>
- Günther T, Schreiner D, Metkar A, Meyer C, Kwade A, Reinhardt G (2020) Classification of calendaring-induced electrode defects and their influence on subsequent processes of lithium-ion battery production. *Energy Technol* 8:1900026. <https://doi.org/10.1002/ente.201900026>
- Mayr A, Schreiner D, Stumper B, Daub R (2022) In-line sensor-based process control of the calendaring process for lithium-ion batteries. *Procedia CIRP* 107:295–301. <https://doi.org/10.1016/j.procir.2022.04.048>
- Mayer D, Schwab B, Fleischer J (2023) Influence of electrode corrugation after calendaring on the geometry of single electrode sheets in battery cell production. *Energy Technol* 11:2200870. <https://doi.org/10.1002/ente.202200870>
- Abdollahifar M, Cavers H, Scheffler S, Diener A, Lippke M, Kwade A (2023) Insights into influencing electrode calendaring on the battery performance. *Adv Energy Mater*. <https://doi.org/10.1002/aenm.202300973>
- Rammerstorfer FG (2018) Buckling of elastic structures under tensile loads. *Acta Mech* 229:881–900. <https://doi.org/10.1007/s00707-017-2006-1>
- Bold B, Fleischer J (2018) Kalandrieren von Elektroden für Li-Ionen-Batterien. *ZWF* 113:571–575. <https://doi.org/10.3139/104.111968>
- Wurba A-K, Klemens J, Mayer D, Reusch C, Altmann L, Leonet O, Blázquez AJ, Boyano I, Ayerebe E, Scharfer P, Schabel W, Fleischer J (2023) Methodology for the characterization and understanding of longitudinal wrinkling during calendaring of lithium-ion and sodium-ion battery electrodes. *Procedia CIRP* 120:314–319. <https://doi.org/10.1016/j.procir.2023.08.056>
- Jacques N, Elias A, Potier-Ferry M, Zahrouni H (2007) Buckling and wrinkling during strip conveying in processing lines. *J Mater Process Technol* 190:33–40. <https://doi.org/10.1016/j.jmatprotec.2007.03.117>
- Friedl N, Rammerstorfer F, Fischer F (2000) Buckling of stretched strips. *Comput Struct* 78:185–190. [https://doi.org/10.1016/S0045-7949\(00\)00072-9](https://doi.org/10.1016/S0045-7949(00)00072-9)
- Jones DP (2021) A new approach to predicting web wrinkling. *Proceedings of the 2021 International Conference on Micro- and Nano-devices Enabled by R2R Manufacturing*, 2021,

- <https://nascent.utexas.edu/sites/default/files/Jones-19-TA2.3.pdf>, accessed 5 November 2023
14. Chen K-S, Ou K-S, Liao Y-M (2011) On the influence of roller misalignments on the web behavior during roll-to-roll processing. *J Chin Inst Eng* 34:87–97. <https://doi.org/10.1080/02533839.2011.552979>
 15. Grima Cintas P (2012) *Industrial statistics with Minitab*. Wiley, Chichester. <https://doi.org/10.1002/9781118383773>
 16. Davim JP (2015) *Design of experiments in production engineering*. Springer, Cham. <https://doi.org/10.1007/978-3-319-23838-8>
 17. Meyer C, Weyhe M, Haselrieder W, Kwade A (2020) Heated calendering of cathodes for lithium-ion batteries with varied carbon black and binder contents. *Energy Technol* 8:1900175. <https://doi.org/10.1002/ente.201900175>
 18. Mayer D, Wurba A-K, Bold B, Bernecker J, Smith A, Fleischer J (2021) Investigation of the mechanical behavior of electrodes after calendering and its influence on singulation and cell performance. *Processes* 9(11):2009. <https://doi.org/10.3390/pr9112009>
 19. Billot N, Günther T, Schreiner D, Stahl R, Kranner J, Beyer M, Reinhart G (2020) Investigation of the adhesion strength along the electrode manufacturing process for improved lithium-ion anodes. *Energy Technol* 8:1801136. <https://doi.org/10.1002/ente.201801136>
 20. Knapieński M (2006) The numerical analysis of roll deflection during plate rolling. *J Mater Process Technol* 175:257–265. <https://doi.org/10.1016/j.jmatprotec.2005.04.051>

Publisher's Note Springer Nature remains neutral with regard to jurisdictional claims in published maps and institutional affiliations.